CHAPTER 5

INFLUENCE OF B_2O_3 ON ELECTRICAL PROPERTIES AND PHASE TRANSITION OF LEAD-FREE $Ba(Ti_{0.9}Sn_{0.1})O_3$ CERAMICS

The phase transition and electrical properties of $Ba(Ti_{0.9}Sn_{0.1})O_3$ ceramics with B_2O_3 added were investigated to explore the effect of B_2O_3 addition on enhanced densification and dielectric constant of these ceramics. With increasing B_2O_3 content, a linear reduction of ferroelectric to paraelectric transition temperature was observed. In addition, higher B_2O_3 concentrations enhanced a ferroelectric relaxor behavior in the ceramics. Changes in this behavior were related to densification, second-phase formation and compositional variation of the ceramics.

5.1 Introduction

In recent years, $BaTiO_3$-based ceramics have received considerable attention from many researchers due to their enhanced electrical performances and environmentally friendly nature leading to their use as a replacement for lead-based ceramics such as $Pb(Zr,Ti)O_3$(PZT) [1-6]. Among the $BaTiO_3$-based ceramics, barium stannate titanate ($BaTi_{1-x}Sn_xO_3$, BTS) ceramics are of particular importance for electronic materials and have been heavily investigated for many years [7-10]. This material has a perovskite-type structure and beneficial electrical properties such as a large dielectric constant and high dielectric tunability [8-11].

The transition temperature from a ferroelectric (FE) to paraelectric (PE) state of barium titanate stannate (BTS) can be controlled by varying the Sn concentration [7]. This material also exhibits a diffuse phase transition and shows a relaxor ferroelectric behavior for some compositions [8, 9]. Since BTS also has a non-toxic composition, it is a promising candidate as an environmentally friendly alternative to the traditional more toxic materials.

For multilayer capacitor applications, many researchers have focused on improving the sintering behaviors and the dielectric properties by adding additives to such $BaTiO_3$-based ceramics [12-16]. Valant and Suvorov [15] studied the effect of Li_2O on the properties of $Ba_{0.6}Sr_{0.4}TiO_3$ ceramics. Although the densification of their ceramics was improved, Li_2O had only a small effect on the transition temperature.

Rhim et al. [13, 14] reported that B_2O_3 helped to increase the dielectric constant of $Ba_{0.7}Sr_{0.3}TiO_3$ ceramics. Further, Qi et al. [16] found that the positive temperature coefficient resistivity (PTCR) effect in $BaTiO_3$-based ceramics was improved by B_2O_3 vapor doping. However, the effects of B_2O_3 addition on phase transition and electrical properties such as dielectric, ferroelectric, and piezoelectric properties of BTS ceramics have not been widely investigated.

It is expected that the electrical properties of BTS ceramics should be improved by B_2O_3 doping. Therefore, the present work was aimed at studying the effects of B_2O_3 on the properties of BTS ceramics. BTS ceramics of the composition $Ba(Ti_{0.9}Sn_{0.1})O_3$ were doped with B_2O_3 and prepared by a solid state reaction to investigate their electrical properties.

5.2 Experimental

Ceramics of $Ba(Ti_{0.9}Sn_{0.1})O_3$, BTS10, were prepared via the conventional method. BTS10 powder was produced by the mixed-oxide technique using reagent grade $BaCO_3$, SnO_2, and TiO_2. The starting powders were then mixed and ball-milled in isopropanol for 24 h using zirconia grinding media. After mixing, the slurry was dried, sieved and calcined for 2h at 1300°C. B_2O_3 powder, equivalent to 1.0, 2.0, and 3.0 wt.%, was then blended to calcined BTS10 powder. The mixed powders, with the addition of polyvinyl alcohol as an organic binder, were then ball-milled in isopropanol for 24 h. This slurry was dried at 150°C and sieved to form a fine powder which was pressed at 100 MPa into 15 mm diameter pellets. The pellets were then sintered at 1350°C for 4h with a heating/cooling rate of 5°C/min after binder burnout at 500°C for 1h.

Phase formation of the sintered samples was checked using a Bruker D8 Advance diffractometer with a Cu-Ka source. The sintered ceramics were also crushed into powders for an X-ray diffraction (XRD) experiment. The dielectric properties and phase transition behaviors were studied at frequencies of 1-500 kHz in the temperature range from -20°C to 100°C using a dielectric measurement system consisting of a HP 4276A LCZ meter and a furnace tube. Polarization was also measured as a function of electric field, using a Sawyer–Tower circuit. Finally, the piezoelectric coefficients (d_{33}) were measured using a PM-3001 d_{33} piezometer. Before the d_{33} measurement was performed, the samples were left for 24 h after poling at 1.5 kV cm^{-1}.

5.3 Results and discussion

5.3.1 Phase formation and densification

The XRD patterns for the sintered ceramic powders containing B_2O_3 up to 3.0 wt.% are shown in Figure 5.1. The XRD results reveal that the main phase of the samples has a perovskite structure. However, a single-phase perovskite was observed for unmodified and 1.0 wt.% samples and small amounts of $BaTi_4O_9$ and $BaTi_5O_{11}$ were found in the 2.0 wt.% sample. In the case of higher B_2O_3 concentrations (3.0 wt.%), another phase of $Ba_2Ti_9O_{20}$ occurred. These results indicate that increased B_2O_3 addition promoted the formation of secondary phases which may in turn produce a change in composition of the samples. Wang et al. [17] reported that $Ba_2Ti_9O_{20}$ could be formed by adding B_2O_3 in a mixture phase of $BaTi_4O_9$ and $BaTi_5O_{11}$. In the present work, the higher B_2O_3 addition may help the $BaTi_4O_9$ and $BaTi_5O_{11}$ components (occurred in the 2.0wt.% sample) transform to $Ba_2Ti_9O_{20}$, which presented the 3.0 wt.% sample.

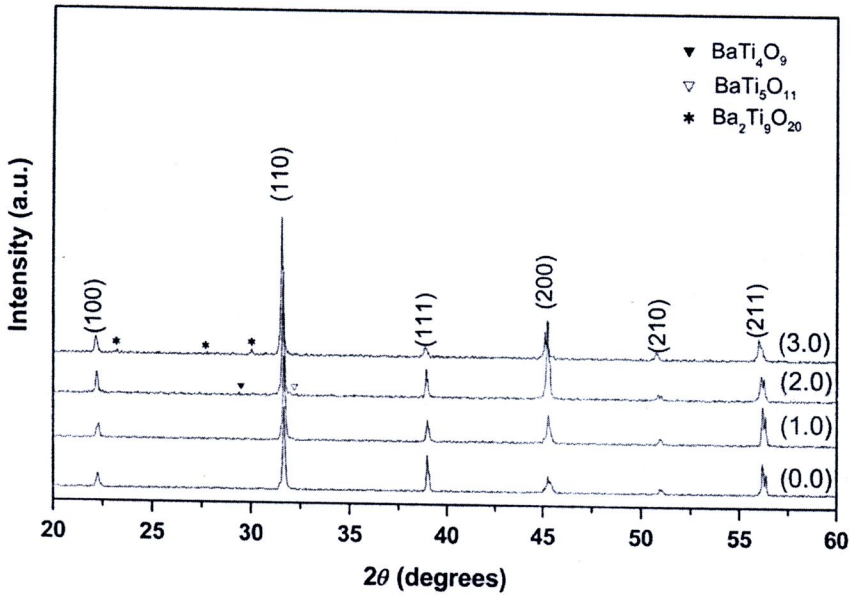

Figure 5. 1 XRD patterns at room temperature of BTS10 ceramics as a function of B_2O_3 content.

From Figure 5.1, the shift in the XRD peak position with increasing B_2O_3 addition indicates a change in lattice parameter. Variation in cell dimensions with B_2O_3 addition was calculated using an equivalent cubic cell parameter corresponding to the unit cell volume as a pseudo-cubic [10, 18]. A plot of the lattice parameter as a function of B_2O_3 addition is shown in Figure 5.2. An increase in lattice parameter with increasing B_2O_3 addition was observed. This implies a lattice distortion in the modified samples.

The sintered density values of the samples for various B_2O_3 content are shown in Figure 5.3. The density increases from 5.231 g cm^{-3} for the unmodified sample to 5.681 g cm^{-3} for the 2.0 wt.% sample then decreased to 5.380 g cm^{-3} for the 3.0 wt.% sample.

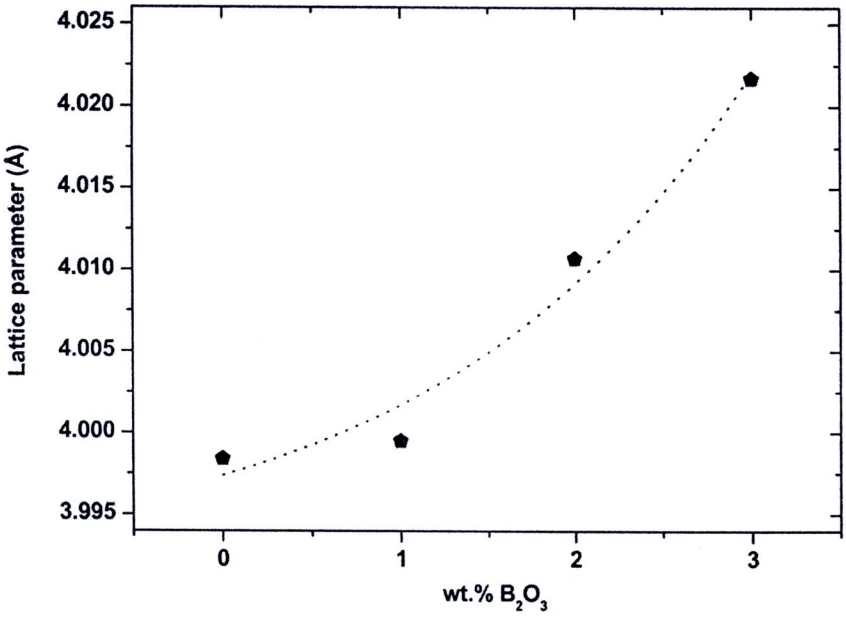

Figure 5. 2 Variation of lattice parameter as a function of B_2O_3 content.

It is known that B_2O_3 can be melted at a low temperature (~ 450°C). Therefore, the B_2O_3 may have formed a liquid phase at a relative low temperature, which promoted sintering [17]. However, it is believed that solid-state sintering becomes dominant and assists the densification at a high temperature. In this work, the optimized amount of B_2O_3 addition for obtaining an optimum density is 2.0 wt.%. An over doping of B_2O_3 (3.0 wt.%) may have caused a higher porosity due to the formation of the another phase. A similar result was reported in a previous work [19].

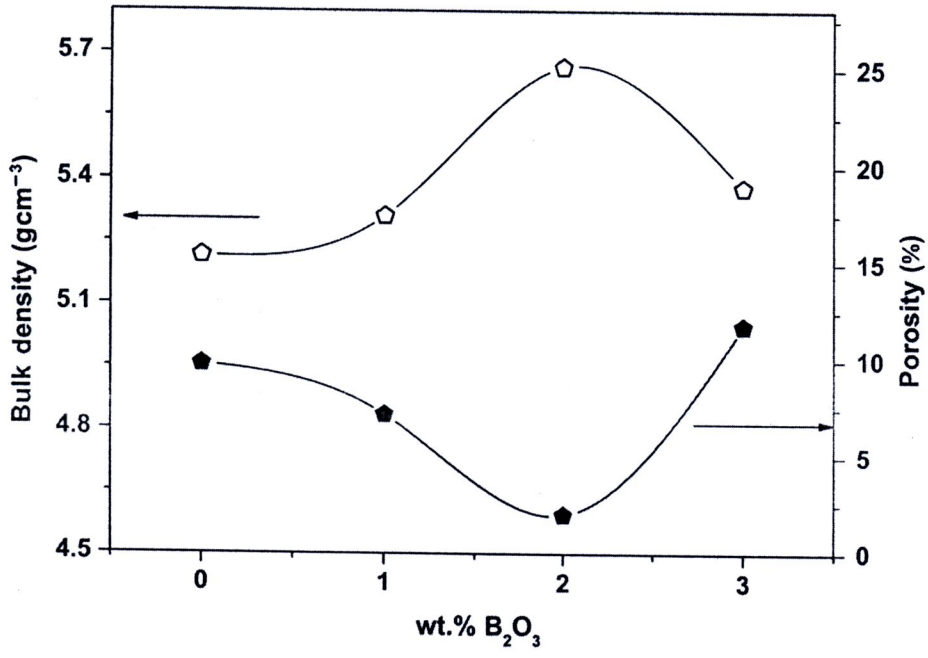

Figure 5. 3 Density and porosity of sintered samples as a function of B_2O_3 content.

5.3.2 Dielectric properties

Figure 5.4 shows the dielectric constant and dielectric loss of the samples as a function of temperature. The dielectric data reveals that B_2O_3 addition has a significant effect on the dielectric constant. The values of the dielectric constant at the dielectric peak ($\varepsilon_{r,max}$) as a function of B_2O_3 content are shown in Figure 5.5. The maximum value of $\varepsilon_{r,max}$ of 13,900 is ~ 46% higher than that of the undoped dielectric constant in the samples depict a was recorded for the 2.0 wt.% sample, which sample. The temperature dependences of the frequency dispersion of the dielectric peak. For the unmodified sample, weak frequency dispersion behavior was observed.

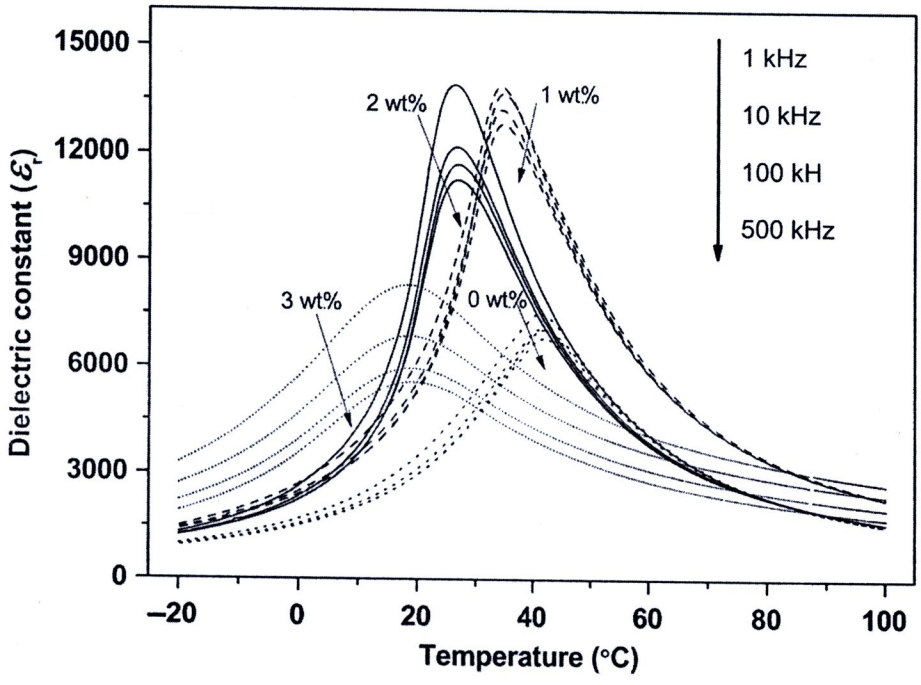

Figure 5. 4 Dielectric constant versus temperature for BTS10 ceramics with differing amounts of B_2O_3 contents.

However, an enhancement of frequency dependence of the dielectric constant was found for higher B_2O_3 contents. The frequency dependence of higher doped samples (2-3 wt.% samples) is also stronger than that in [9] for the same composition. This implies that ferroelectric relaxor behavior was enhanced. It should be noted that the value of the dielectric constant for the 1.0 wt.% sample was found to be close to the value obtained for the 2.0wt.% sample, which is unexpected because the 2.0 wt.% sample has the maximum density. This result may be due to the existence of a second phase in the 2.0 wt.% sample which deteriorated the dielectric constant. For higher B_2O_3 concentrations (3.0wt.%), the sample presented a lower dielectric constant, which may be due to the presence of another phase and higher porosity.

Values of the dielectric loss (tanδ) of undoped and doped ceramics are shown in Table 5.1. The tanδ at room temperature (denote as tanδ_{room}) and at $\varepsilon_{r,max}$ (denote as tanδ_{max}) has a trend to increase with B_2O_3 content. However, high tanδ_{room} and tanδ_{max} (~ 40.1) was observed for 2.0 and 3.0wt.% sample, implying that these samples have lower resistivity.

Table 5. 1 Electrical properties of B_2O_3 doped BTS10 ceramics.

Amount of B_2O_3 (wt.%)	$\varepsilon_{r,room}$	tanδ_{room}	$\varepsilon_{r,room}$	tanδ_{room}	δ_f (°C)	P_r (μC cm^2)	E_c (kV cm)	d_{33} (pC N^{-1})
0.0	4400	0.085	7500	0.045	15.8	1.1138	0.271	104
1.0	8400	0.069	13800	0.035	16.1	1.6600	0.383	107
2.0	13800	0.123	13900	0.115	14.0	1.6968	0.542	Break down
3.0	7700	0.155	8300	0.178	280.1	0.9448	0.568	Break down

5.3.3 Phase transition studies

The transition temperature (T_m) at the dielectric maximum peak of the dielectric curve ($\varepsilon_{r,max}$) as a function of B_2O_3 concentration is shown in Figure 5.5. The T_m at the dielectric peak was observed to decrease linearly from 41°C for the unmodified sample to 18°C for the 3.0 wt.% sample. This result indicates that the Tm of this system can be controlled by the addition of B_2O_3. In this work, lattice distortion and compositional variation may be the major reasons for this behavior. It was suggested from the literature that B ions can act as interstitial ions in $BaTiO_3$ lattice due to their very small ionic radius which can cause a lattice distortion [16]. Although the structure of $Ba(Ti_{0.9}Sn_{0.1})O_3$ in this work is complex compared to

$BaTiO_3$ and it has a symmetry close to cubic, it is believed that some B ions can be incorporated into lattices.

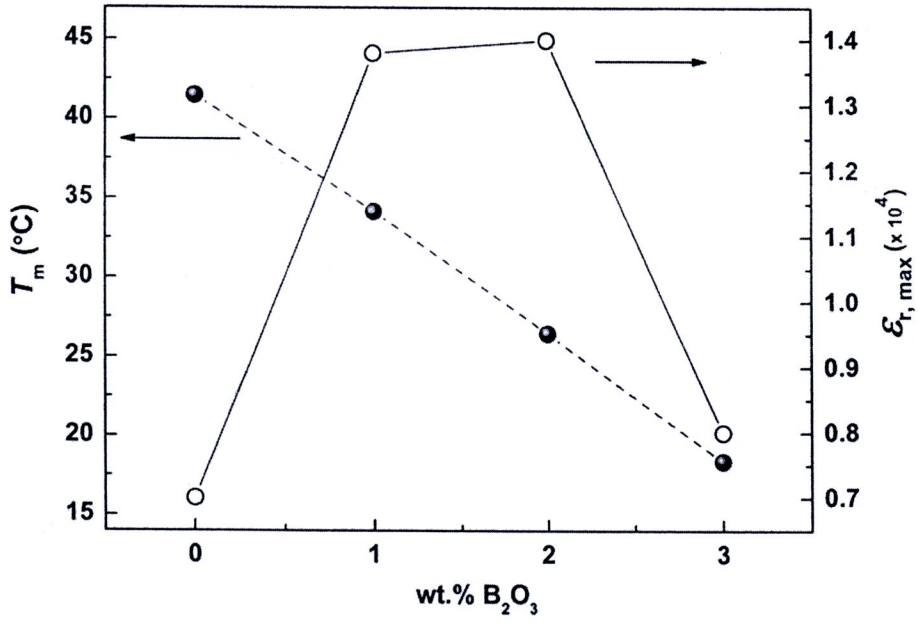

Figure 5. 5 Transition temperature (T_m) and maximum dielectric constant ($\varepsilon_{r,max}$) of the ceramics as a function of B_2O_3 content.

The incorporation of B ions may produce lattice distortion and defects at A sites in the samples[16]. Furthermore, a second-phase formation in the sample may cause the compositional variation. These changes may also have produced a difference in local transition temperatures, resulting in the shift of T_m [20]. It has been suggested that the paraelectric side of the permittivity curve, having diffuse phase transition, can be written as [21]

$$\frac{\varepsilon_{r,max}}{\varepsilon_r} = exp\left[\frac{(T - T_m)^2}{2\delta_\gamma^2}\right] \tag{5.1}$$

where $\varepsilon_{r,max}$ is maximum value of the relative permittivity at transition temperature (T=T_m); ε_r is the dielectric constant of sample; and δ_γ is diffuseness parameter of the transition. The value of δ_γ can be calculated from $ln(\varepsilon_{r,max}/\varepsilon_r)$ versus $(T-T_m)^2$ curve [22]. This value is valid for the range of $(\varepsilon_{r,max}/\varepsilon_r) < 1.5$, as clarified by Pilgrim et al. [21]. The values of parameter δ_γ for various B_2O_3 contents are listed in Table 1. The parameter δ_γ was laid between 14.0 and 28.1 K. The lower value of δ_γ was observed in the 2.0 wt.% sample, indicating that 2.0 wt.% B_2O_3 addition promoted a sharper phase transition in the $Ba(Ti_{0.9}Sn_{0.1})O_3$ system.

5.3.4 Ferroelectric and piezoelectric properties

In the present work, the ferroelectric properties of the ceramics were measured using a Sawyer–Tower circuit at room temperature. The hysteresis loops (P-E) for various B_2O_3 contents are shown in Figure 5.6. All samples showed a slim ferroelectric hysteresis loop. Ferroelectric properties including the saturated polarization (P_r), and coercive field (E_c) are listed in Table 5.1. A slight change in the ferroelectric properties was observed for the 1.0-2.0 wt.% samples. For the 3.0 wt.% sample, the hysteresis loop became more slanted with a lower P_r value. The existence of a ferroelectric hysteresis loop above the transition temperature (~ 18°C) for the 3.0 wt.% sample, indicates a relaxor behavior which confirms the dielectric result [23]. It should be noted that higher B_2O_3 samples showed an unsaturated hysteresis loop. Previous work suggested that [24, 25] the unsaturated hysteresis loop could be related to a high leakage current.

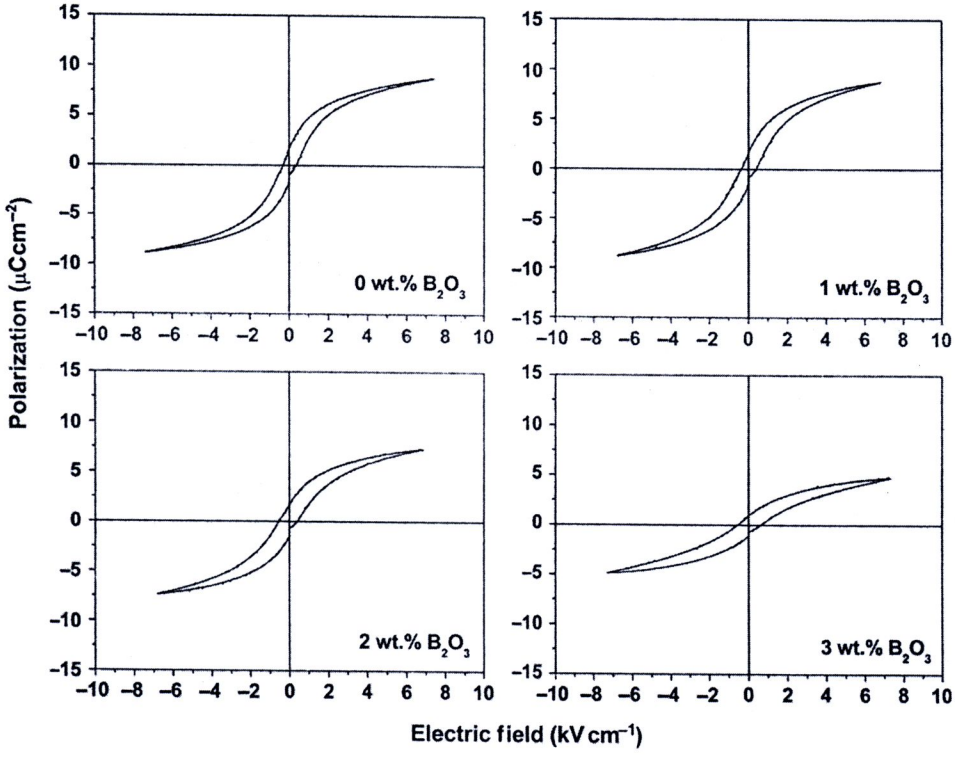

Figure 5. 6 Dependence of the polarization versus electric field (*P-E*) loop on the B_2O_3 dopant concentration.

To check this possibility, the leakage current densities of the samples were measured. A plot of leakage current density as a function of applied voltage and annealing time is displayed in Figure 5.7. Higher leakage current densities were observed for longer annealed samples, as expected. This result is thus confirmed that the high B_2O_3 content samples have lower resistivity.

Therefore, samples with 2.0 and 3.0wt.% B_2O_3 exhibited lower dielectric strengths. These samples can easily break down in the poling process. However, the d_{33} values were measured to be 104 and 107 pC N^{-1} for the undoped and 1.0 wt.% samples, respectively (Table 5.1).

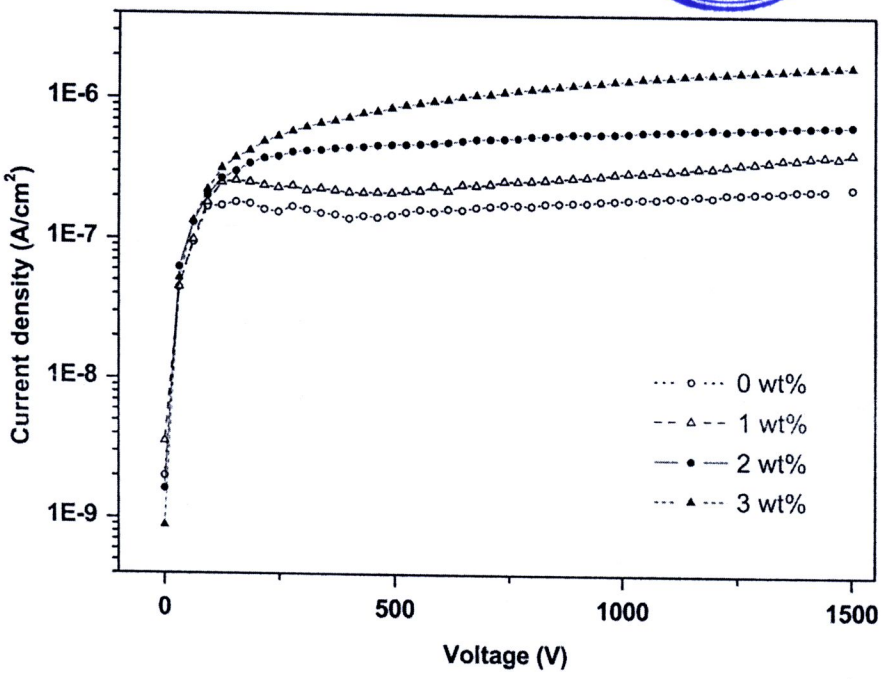

Figure 5. 7 Leakage current density as a function of voltage for B_2O_3-doped BTS10 ceramics.

In this work some mechanical property such as hardness was also investigated due to an important from some application viewpoint that this ceramics are resistant to fracture or microcracking when subjected to large electric fields. The result of hardness measurements is shown in Figure 5.8. It was found that B_2O_3 addition has a significant effect on the enhancement of Vickers hardness values. A linear increase in the hardness was observed which can be expressed by the following equation;

$$H_V = 2.16 + 0.45[B_2O_3] \quad (5.2)$$

where H_V is Vickers hardness and $[B_2O_3]$ is B_2O_3 concentration. This result indicates that B_2O_3 help to improve the mechanical property of the ceramics. It is possible that partial amount of B_2O_3 might deposit to grain or grain boundaries and resist to the

crack that pass through the grain and grain boundary as a result of the increase in the hardness value due to its high mechanical properties [26].

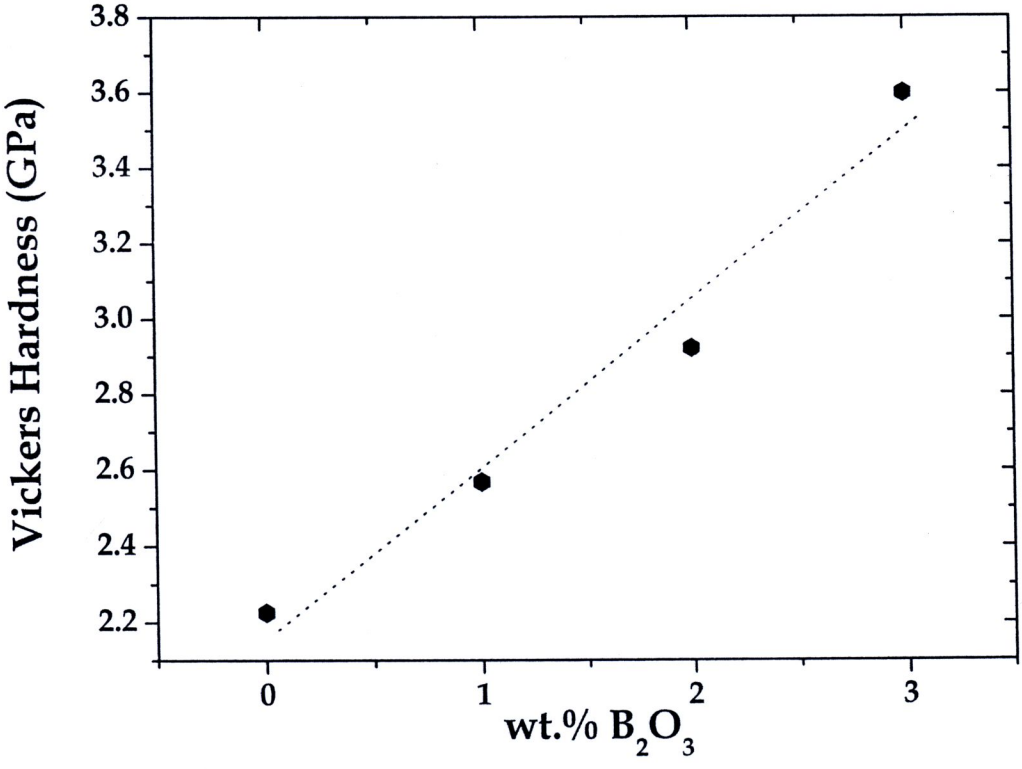

Figure 5. 8 Variation of Vickers hardness number with B_2O_3 content.

5.4 Conclusions

In the present work, we demonstrated that B_2O_3 has significant effects on the electrical properties and phase transition behavior of $Ba(Ti_{0.9}Sn_{0.1})O_3$ ceramics. The density and dielectric constant were enhanced by adding B_2O_3 up to 2.0wt.%. This dielectric result indicates that high B_2O_3 content produced a reduction in the FE–PE transition temperatures. In addition, B_2O_3 addition enhanced the ferroelectric relaxor

behavior and the hardness in the ceramics. The result may be useful in the development of multi-layer capacitor applications.

5.5 References

[1] A.J. Moulson, J.M. Herbert, Wiley InterScience (Online service), Electroceramics : materials, properties, applications, in, J. Wiley,, New York, 2003, pp. 557 p. ill.

[2] T. Shrout, S. Zhang, Lead-free piezoelectric ceramics: Alternatives for PZT, Journal of Electroceramics, 19 (2007) 113-126.

[3] M. Kumar, A. Garg, R. Kumar, M.C. Bhatnagar, Structural, dielectric and ferroelectric study of $Ba_{0.9}Sr_{0.1}Zr_xTi_{1-x}O_3$ ceramics prepared by the sol–gel method, Physica B: Condensed Matter, 403 (2008) 1819-1823.

[4] C.R.K. Mohan, P.K. Bajpai, Effect of sintering optimization on the electrical properties of bulk $Ba_xSr_{1-x}TiO_3$ ceramics, Physica B: Condensed Matter, 403 (2008) 2173-2188.

[5] P. Jarupoom, K. Pengpat, N. Pisitpipathsin, S. Eitssayeam, U. Intatha, G. Rujijanagul, T. Tunkasiri, Development of electrical properties in lead-free bismuth sodium lanthanum titanate–barium titanate ceramic near the morphotropic phase boundary, Current Applied Physics, 8 (2008) 253-257.

[6] K. Pengpat, S. Hanphimol, S. Eitssayeam, U. Intatha, G. Rujijanagul, T. Tunkasiri, Morphotropic phase boundary and electrical properties of lead-free bismuth sodium lanthanum titanate—barium titanate ceramics, Journal of Electroceramics, 16 (2006) 301-305.

[7] J.N. Lin, T.B. Wu, Effects of isovalent substitutions on lattice softening and transition character of $BaTiO_3$ solid solutions, Journal of Applied Physics, 68 (1990) 985-993.

[8] W. Xiaoyong, F. Yujun, Y. Xi, Dielectric relaxation behavior in barium stannate titanate ferroelectric ceramics with diffused phase transition, Applied Physics Letters, 83 (2003) 2031-2033.

[9] V.V. Shvartsman, J. Dec, Z.K. Xu, J. Banys, P. Keburis, W. Kleemann, Crossover from ferroelectric to relaxor behavior in $BaTi_{1-x}Sn_xO_3$ solid solutions, Phase Transitions, 81 (2008) 1013-1021.

[10] Z. Jiwei, S. Bo, Y. Xi, Z. Liangying, Dielectric and ferroelectric properties of $Ba(Sn_{0.15}Ti_{0.85})O_3$ thin films grown by a sol–gel process, Materials Research Bulletin, 39 (2004) 1599-1606.

[11] J. Zhai, B. Shen, X. Yao, L. Zhang, H. Chen, Dielectric properties of $Ba(Sn_xTi_{1-x})O_3$ thin films grown by a sol–gel process, Journal of the American Ceramic Society, 87 (2004) 2223-2227.

[12] D. Prakash, B.P. Sharma, T.R. Rama Mohan, P. Gopalan, Flux additions in barium titanate: Overview and prospects, Journal of Solid State Chemistry, 155 (2000) 86-95.

[13] S.M. Rhim, S. Hong, H. Bak, O.K. Kim, Effects of B_2O_3 addition on the dielectric and ferroelectric properties of $Ba_{0.7}Sr_{0.3}TiO_3$ ceramics, Journal of the American Ceramic Society, 83 (2000) 1145-1148.

[14] S.M. Rhim, H. Bak, S. Hong, O.K. Kim, Effects of heating rate on the sintering behavior and the dielectric properties of $Ba_{0.7}Sr_{0.3}TiO_3$ ceramics prepared by boron-containing liquid-phase sintering, Journal of the American Ceramic Society, 83 (2000) 3009-3013.

[15] M. Valant, D. Suvorov, Low-temperature sintering of $(Ba_{0.6}Sr_{0.4})TiO_3$, Journal of the American Ceramic Society, 87 (2004) 1222-1226.

[16] Q. Jianquan, Z. Qing, W. Yongli, W. Yajing, L. Longtu, Enhancement of positive temperature coefficient resistance effect of $BaTiO_3$-based semiconducting ceramics caused by B_2O_3 vapor dopants, Solid State Communications, 120 (2001) 505-508.

[17] S.-F. Wang, C.-C. Chung, C.-H. Wang, J.P. Chu, Effects of B_2O_3 on the phase stability of $Ba_2Ti_9O_{20}$ microwave ceramic, Journal of the American Ceramic Society, 85 (2002) 1619-1621.

[18] Y.L. Tu, J.M. Herbert, S.J. Miline, Fabrication and characterization of high permittivity ceramics in the $Ba(Ti_{1-x-y}Sn_xZr_y)O_3$ system, Journal of Materials Science, 29 (1994) 4152-4156.

[19] C.-L. Huang, Y.-B. Chen, C.-F. Tasi, Influence of B_2O_3 additions to $0.8(Mg_{0.95}Zn_{0.05})TiO_3$-$0.2Ca_{0.61}Nd_{0.26}TiO_3$ ceramics on sintering behavior and microwave dielectric properties, Journal of Alloys and Compounds, 460 (2008) 675-679.

[20] P.V. Divya, V. Kumar, Crystallization studies and properties of $(Ba_{1-x}Sr_x)TiO_3$ in borosilicate glass, Journal of the American Ceramic Society, 90 (2007) 472-476.

[21] S.M. Pilgrim, A.E. Sutherland, S.R. Winzer, Diffuseness as a useful parameter for relaxor ceramics, Journal of the American Ceramic Society, 73 (1990) 3122-3125.

[22] G. Rujijanagul, N. Vittayakorn, Influence of fabrication processing on phase transition and electrical properties of $0.8Pb(Zr_{1/2}Ti_{1/2})O_3–0.2Pb(Ni_{1/3}Nb_{2/3})O_3$ ceramics, Current Applied Physics, 8 (2008) 88-92.

[23] Z. Wang, X. Li, X. Long, Z.-G. Ye, Characterization of relaxor ferroelectric behavior in the $(1–x)Ba(Yb_{1/2}Nb_{1/2})O_3–xPbTiO_3$ solid solution, Scripta Materialia, 60 (2009) 830-833.

[24] S.K. Singh, K. Maruyama, H. Ishiwara, Reduced leakage current in La and Ni codoped $BiFeO_3$ thin films, Applied Physics Letters, 91 (2007) 112913-112913.

[25] X. Wang, H. Liu, B. Yan, Enhanced ferroelectric properties of Ce-substituted $BiFeO_3$ thin films on $LaNiO_3$/Si substrates prepared by sol–gel process, Journal of the European Ceramic Society, 29 (2009) 1183-1187.

[26] D. Buc, I. Bello, M. Caplovicova, M. Mikula, J. Kovac, I. Hotovy, Y.M. Chong, G.G. Siu, Analysis of magnetron sputtered boron oxide films, Thin Solid Films, 515 (2007) 8723-8727.